1960

Random neutron flux variations in a subcritical assembly.

Rough, Jimmie Lynn
Iowa State University

RANDOM NEUTRON FLUX VARIATIONS IN A SUBCRITICAL ASSEMBLY

JIMMIE LYNN ROUGH

RANDOM NEUTRON FLUX VARIATIONS

IN A SUBCRITICAL ASSEMBLY

by

Jimmie Lynn Hough

A Thesis Submitted to the

Graduate Faculty in Partial Fulfillment of

The Requirements for the Degree of

MASTER OF SCIENCE

Major Subject: Nuclear Engineering

TABLE OF CONTENTS

INTRODUCTION

The subcritical assembly has been used as an educational device to demonstrate the principles of nuclear science and engineering, and for research in experimental reactor engineering. There are several advantages in the use of a subcritical assembly. The assembly is small in size and relatively inexpensive in materials, construction, and required apparatus. Only nominal shielding is required due to the low activity involved. Lattice parameters can be varied more easily than in a critical assembly.

The kinetic equations of the assembly are time dependent, non-linear differential equations which may be linearized in the derivation of the transfer function. The method of experimental evaluation of the transfer function is to vary one or more of the parameters in such a way that the limits within which the linearization is valid are not exceeded. This variation of the parameters is called "forcing". The usual methods of forcing in a subcritical assembly are varying the strength of the neutron source or the reactivity in a periodic manner. The minimum periodic input signal to which the response can be measured is determined by the amplitude of the random or stochastic variations in the steady state flux level due to the inherent statistical nature of the fission process. It is possible, in a system with large stochastic variations in the neutron flux, to exceed the range of line-

arity of the kinetic equations by making the magnitude of the input signal large enough to obtain a readable response. A technique has been developed, from studies of stochastic processes such as Brownian Motion, which makes it possible to evaluate the transfer function of an assembly. The stochastic or random variation in the flux is considered to be the response of the system to stochastic source forcing due to the statistical nature of the basic phenomena involved. This method of evaluation of the transfer function should be least likely to invalidate the linear approximations made.

REVIEW OF THE LITERATURE

A great amount of effort has been expended in the derivation and evaluation of critical assembly transfer functions. One of the primary reasons was the need for an automatic control system to maintain a given power level in a reactor. The similarity of the transfer function of a reactor to that of a servomechanism control system had been noted, and it was determined that this type of system was suitable for reactor control.

Owens, Crever, and Pigott (13) in 1949 proposed the concept of treating a critical assembly as a "black box" to which a feedback control system could be applied in order to maintain a desired power level. The proposal was based on the observation that the roots of the kinetic equation of the assembly were negative. This indicated that the critical assembly transfer function was the same as the transfer function for a minimum phase shift network, and that the transfer characteristic could be represented by a Bode diagram. In that same year Franz (5) presented a more detailed derivation of the transfer function and showed that the standard techniques of servomechanism theory applied. Harrer, Boyar, and Krucoff (9) evaluated the transfer function of the CP-2 reactor by sinusoidally varying the reactivity, and showed that the transfer function could be used in the design of servo loops or regulating systems which include the reactor.

Mockup assemblies have been utilized for the determination of the transfer function of proposed reactors. Boland, Smith, and Rice (3) measured the zero power transfer function of a fast critical assembly, ZPR-III mockup assembly of EBR-I, Mark III, by determining the change in power level due to oscillation of the reactivity.

Refinement in the techniques of testing and the evaluation of transfer functions are constantly sought, and the subcritical assembly provides a relatively simple vehicle for such investigations. A subcritical assembly was utilized by Axtmann, Dessauer, and Parkinson (1) for reactivity measurements and testing of pile components. The transfer function of the Iowa State University subcritical assembly was initially evaluated by Ricci (14) utilizing the method of source forcing.

A new technique for evaluation of the transfer function of a nuclear reactor operating at a steady state by an analysis of the random, or stochastic, nature of the neutron population has been developed recently. Moore (11) has shown mathematically that the square of the modulus of the transfer function of a reactor is proportional to the Fourier transform of the autocorrelation function which is equal to the power spectral density function of the system. This was verified experimentally by Cohn (4) and by Griffin and Lundholm (8). Vélez (16) evaluated the transfer function of the Ford Nuclear

Reactor and the subcritical assembly at the University of Michigan by the direct measurement of the autocorrelation function, but the results were reported to be inconclusive in the case of the subcritical assembly. All references found describing the evaluation of the transfer function by measurement of the power spectral density function pertained to critical assemblies.

DEVELOPMENT OF THE KINETIC EQUATIONS

The kinetic equations of the subcritical assembly can be derived from the general diffusion equation (6, p. 223 and 7, p. 101)

$$D \nabla^2 \phi - \Sigma_a \phi + S = \frac{\partial n}{\partial t} = \frac{1}{v} \frac{\partial \phi}{\partial t} \qquad (1)$$

which is applicable to that region of a subcritical assembly away from the extraneous neutron source where most of the neutrons are fission neutrons. The symbols used are defined in the table of symbols. The first term represents the loss of thermal neutrons due to leakage from the assembly; the second term is the loss of thermal neutrons due to absorption; the third term is the neutron production or source term; and the right side of the equation is the non-equilibrium change in neutron population with time.

The source term is made up of prompt and delayed fission neutrons, and neutrons from an external source. It has been shown (7, p. 193) that the number of fast fission neutrons produced is $\frac{k_\infty}{p} \Sigma_a \phi$, and further (6, p. 226) that if β is the total fraction of delayed neutrons the prompt neutron source term S_p is

$$S_p = (1 - \beta) k_\infty \Sigma_a \phi \, e^{-B^2 \tau} \qquad (2)$$

There are six known groups of delayed neutrons that account for 0.64 per cent of the thermal neutron production.

These delayed neutrons accompany the radioactive decay of certain fission products, called neutron precursors, which exist in an excited state. If β_i is the fraction of each delayed neutron group then the formation of the precursors of the group would be $\beta_i \frac{k_\infty}{p} \Sigma_a \phi$. When the concentration of a precursor group is denoted by c_i and the decay constant as λ_i, the rate of decay would be $\lambda_i c_i$. The net rate of formation of precursors to the i-th delayed neutron group would then be

$$\frac{\partial c_i}{\partial t} = \beta_i \frac{k_\infty}{p} \Sigma_a \phi - \lambda_i c_i \tag{3}$$

The total rate of production of delayed neutrons is $\sum_{i=1}^{6} \lambda_i c_i$, and when multiplied by the resonance escape probability, p, and the slowing down non leakage probability, $e^{-B^2 \tau}$, the result is the delayed thermal neutron source term

$$S_d = p\, e^{-B^2 \tau} \sum_{i=1}^{6} \lambda_i\, c_i \tag{4}$$

Table 1. Table of symbols

B^2	Buckling	$cm.^{-2}$
β	Fraction of delayed neutrons	
β_i	Fraction of i-th group of delayed neutrons	
C	Number of delayed neutron precursors in the assembly	
C_i	Number of the i-th group of delayed neutron precursors in the assembly	

Table 1. (Continued)

c	Concentration of delayed neutron precursors	
c_i	Concentration of i-th group of delayed neutron precursors	
D	Thermal neutron diffusion coefficient	cm.
f	Frequency	$\frac{\text{cycles}}{\text{sec.}}$
k	Effective multiplication factor	
k_∞	Multiplication factor for an infinite assembly	
L	Neutron diffusion length in the moderator	cm.
ℓ^*	Prompt neutron lifetime in a finite assembly	sec.
ℓ_o	Prompt neutron lifetime in an infinite assembly	sec.
ℓ	Average neutron lifetime in a finite assembly	sec.
$\bar{\lambda}$	Average decay constant of delayed neutron precursors	sec.$^{-1}$
λ_i	Decay constant of the i-th group of delayed neutron precursors	sec.$^{-1}$
N	Total number of thermal neutrons in a finite assembly	
n	Number of thermal neutrons per unit volume	$\frac{\text{neutrons}}{\text{cm.}^3}$
p	Resonance escape probability	
ϕ	Thermal neutron flux	$\frac{\text{neutrons}}{\text{cm.}^2\text{sec.}}$
S	Rate of production of thermal neutrons per unit volume from all source	$\frac{\text{neutrons}}{\text{cm.}^3\text{sec.}}$
S_e	Total external thermal neutron source contribution to the assembly	$\frac{\text{neutrons}}{\text{sec.}}$

Table 1. (Continued)

$\mathcal{S}$	External thermal neutron source contribution per unit volume	$\frac{\text{neutrons}}{\text{cm.}^3\text{sec.}}$
Σ_a	Macroscopic absorption cross section	cm.$^{-1}$
t	Time	sec.
τ	Fermi age	cm.^{2}
v	Thermal neutron mean velocity	cm./sec.
ω	Frequency	$\frac{\text{radians}}{\text{sec.}}$

The contribution of the external thermal neutron source term will be assumed to be

$$S = \mathcal{S} \tag{5}$$

Substitution of Equations 2, 4, and 5 into Equation 1 yields

$$\begin{aligned} \frac{\partial n}{\partial t} &= D \nabla^2 \phi - \Sigma_a \phi + (1 - \beta) k_\infty \Sigma_a \phi e^{-B^2 \tau} \\ &\quad + p\, e^{-B^2 \tau} \sum_{i=1}^{6} \lambda_i c_i + \mathcal{S} \end{aligned} \tag{6}$$

ϕ and c_i are functions of space and time, and it can be shown (6, p. 227) that the space and time variables are separable allowing the partial differential equation to be reduced to an ordinary differential equation. Consideration of the fundamental space mode only (6, p. 227 and 9, p. 33) yields

the equality

$$\nabla^2 \phi = - B^2 \phi \tag{7}$$

The diffusion length is defined by

$$L^2 = \frac{D}{\Sigma_a} \tag{8}$$

Rearrangement of the equation yields

$$D = L^2 \Sigma_a \tag{9}$$

The mean life of thermal neutrons in an infinite medium is defined by

$$\ell_o \equiv \frac{\lambda_a}{v} = \frac{1}{\Sigma_a v} \tag{10}$$

When rearranged this relation becomes

$$\Sigma_a = \frac{1}{\ell_o v} \tag{11}$$

The flux, the effective multiplication factor in a finite medium, and the prompt neutron lifetime in a finite medium are defined by

$$\phi = nv \tag{12}$$

$$k = \frac{k_\infty \, e^{-B^2 \tau}}{1 + L^2 B^2} \tag{13}$$

$$\ell^* = \frac{\ell_o}{1 + L^2 B^2} \tag{14}$$

The combination of Equations 13 and 14 yields

$$k_\infty = \frac{\ell_o\, k}{\ell^* e^{-B^2\tau}} \tag{15}$$

The substitution of Equations 7, 9, 11, 12, and 15 into Equation 6 yields

$$\frac{dn}{dt} = -\,(L^2B^2 + 1)\,\frac{n}{\ell_o} + (1-\beta)k\,\frac{n}{\ell^*} + p\, e^{-B^2\tau}\sum_{i=1}^{6}\lambda_i c_i + s \tag{16}$$

The combination of Equation 14 with Equation 16 and rearranging yields

$$\frac{dn}{dt} = [k(1-\beta) - 1]\,\frac{n}{\ell^*} + p\, e^{-B^2\tau}\sum_{i=1}^{6}\lambda_i c_i + s \tag{17}$$

When Equations 11, 12, and 15 are substituted into Equation 3 the result is

$$\frac{dc_i}{dt} = \beta_i\,\frac{k\ n}{pe^{-B^2\tau}\ell^*} - \lambda_i c_i \tag{18}$$

Equations 17 and 18 are the coupled kinetic equations of the subcritical assembly.

It should be noted at this point that in arriving at Equation 17 the assumption has been made that the external source contributes a different number of thermal monoenergetic neutrons to each unit volume of the subcritical assembly, the number decreasing with height in the assembly. The kinetic equations can also be derived by considering the total neutron population rather than the neutron population

on a per unit volume basis.

Consider that at a particular time the assembly contains N neutrons, and the effective reproduction constant, k, is less than one. The prompt neutron lifetime is ℓ^*, the prompt neutron reproduction constant is k_p, and the rate of decrease of neutron population in the assembly is $(k_p - 1)\ N/\ell^*$, if neutrons are not supplied to the assembly from an external source. Absorption and leakage account for the decrease. If β is the fraction of delayed neutrons then the prompt neutron reproduction constant, k_p, can be replaced by $k(1 - \beta)$. The rate of decrease of neutron population with time is then given by

$$\frac{dN}{dt} = \left[k(1 - \beta) - 1\right]\ N/\ell^* \tag{19}$$

Neutrons are supplied to the assembly by an external source and six groups of delayed neutrons. The total number of delayed neutrons of the i-th group stored in the fissions products of the assembly at any time is C_i. If the decay constant of the nuclei containing the i-th group of delayed neutrons is λ_i, the neutrons of that group are emitted at a rate $\lambda_i C_i$ as fast neutrons. These fast delayed neutrons must be corrected for fast non-leakage, $e^{-B^2\tau}$, and resonance escape probability, p. Summation of the terms in the non-equilibrium rate equation for the assembly yields

$$\frac{dN}{dt} = \left[k(1-\beta)-1\right]\frac{N}{\ell^*} + pe^{-B^2\tau}\sum_{i=1}^{6}\lambda_i C_i + S_e \qquad (20)$$

The total number of thermal neutrons being produced per unit time is $\frac{k\,N}{\ell^*}$ of which a fraction β are delayed. The delayed neutrons are not lost by leakage or absorption until after they are emitted from the fission products, and hence the number of delayed neutrons stored in the fission products is greater than $\frac{k\,N}{\ell^*}$ by the factor $\frac{1}{p\,e^{-B^2\tau}}$. The non-equilibrium equation for the i-th group of delayed neutrons is

$$\frac{d\,C_i}{dt} = \frac{\beta_i k\,N}{p\,e^{-B^2\tau}} - \lambda_i\,C_i \qquad (21)$$

Equations 20 and 21 are the same as Equations 17 and 18 except that they are based upon the total number of neutrons in the assembly, and the external source term then accounts for all of the neutrons supplied to the assembly. The neutron flux at any point in the assembly can be considered to be proportional to the total number of neutrons in the assembly at a particular instant. The use of either set of coupled kinetic equations in the derivation of the transfer function will yield the same result.

DERIVATION OF THE TRANSFER FUNCTIONS

The kinetic equations and the resultant transfer function can be varied by varying the source or reactivity in a predetermined manner. This variation is usually sinusoidal when purposely introduced. However, the source strength and reactivity may vary even at "steady state" conditions. This is due to the fluctuation in the number of neutrons available to the assembly caused by the natural statistical fluctuations in the rates of neutron absorption and fission. The resultant random variations in the neutron flux make possible the evaluation of the transfer function by proper analysis at steady state.

Transfer Function with Source Variation

For steady state conditions (using zero subscripts) Equations 17 and 18 become

$$\frac{dn}{dt} = 0 = \left[k(1-\beta)-1\right]\frac{n_o}{\ell^*} + pe^{-B^2\tau}\sum_{i=1}^{6}\lambda_i c_{i_o} + s_o \qquad (22)$$

$$\frac{dc_i}{dt} = 0 = \frac{\beta_i k}{p\,e^{-B^2\tau}} \cdot \frac{n_o}{\ell^*} - \lambda_i\, c_{i_o} \qquad (23)$$

Consider a small variation δs to be superimposed on s_o so that

$$\begin{aligned} s &= s_o + \delta s \\ n &= n_o + \delta n \\ c_i &= c_{i_o} + \delta c_i \end{aligned} \qquad (24)$$

Substitution of Equation 24 into Equations 17 and 18 yields,

$$\frac{dn}{dt} = \frac{d\delta n}{dt} = \left[k(1-\beta) - 1\right]\frac{(n_o + \delta n)}{\ell^*} + pe^{-B^2\tau}\sum_{i=1}^{6}\lambda_i(c_{i_o} + \delta c_i) + s_o + \delta s \tag{25}$$

and

$$\frac{dc_i}{dt} = \frac{d\delta c_i}{dt} = \frac{\beta_i k}{pe^{-B^2\tau}}\ \frac{(n_o + \delta n)}{\ell^*} - \lambda_i(c_{i_o} + \delta c_i) \tag{26}$$

When the terms of Equations 25 and 26 are expanded, the steady state components of Equations 22 and 23 are collected and set equal to zero, the resultant equations are

$$\frac{d\delta n}{dt} = \frac{k-1}{\ell^*}\delta n - \frac{k\beta}{\ell^*}\ \delta n + pe^{-B^2\tau}\sum_{i=1}^{6}\lambda_i\delta c_i + \delta s \tag{27}$$

$$\frac{d\delta c_i}{dt} = \frac{\beta_i k}{p\ell^* e^{-B^2\tau}}\ \delta n - \lambda_i c_i \tag{28}$$

By transforming to Laplace notation Equations 27 and 28 become

$$s\delta n(s) = \frac{k-1}{\ell^*}\ \delta n(s) - \frac{k\beta}{\ell^*}\delta n(s) + pe^{-B^2\tau}\sum_{i=1}^{6}\lambda_i\delta c_i(s) + \delta s(s) \tag{29}$$

$$s\delta c_i(s) = \frac{\beta_i k}{p\ell^* e^{-B^2\tau}}\ \delta n(s) - \lambda_i\ \delta c_i(s) \tag{30}$$

Rearrangement of Equation 30 yields

$$\delta c_i(s) = \frac{\beta_i k}{p\ell^* e^{-B^2\tau}}\ \frac{1}{s + \lambda_i}\ \delta n(s) \tag{31}$$

Substitution of Equation 31 in Equation 29 and collecting terms yields

$$\delta n(s)\left\{ s - \frac{k-1}{\ell^*} + \frac{k\beta}{\ell^*} - \sum_{i=1}^{6} \frac{\beta_i \lambda_i k}{\ell^*(s+\lambda_i)}\right\} = \delta \mathscr{k}(s) \qquad (32)$$

By rearranging Equation 32, the transfer function becomes

$$\frac{\delta n(s)}{\delta \mathscr{k}(s)} = \frac{\ell^*}{s\ell^* - k + 1 + k\beta - k\sum_{i=1}^{6}\frac{\beta_i \lambda_i}{s+\lambda_i}} \qquad (33)$$

By substitution of $\frac{\bar{\lambda}\beta}{s+\bar{\lambda}}$ for $\sum_{i=1}^{6}\frac{\beta_i \lambda_i}{s+\lambda_i}$ Equation 33 becomes

$$\frac{\delta n(s)}{\delta \mathscr{k}(s)} = \frac{\ell^*}{s\ell^* - k(1-\beta) + 1 - k\frac{\bar{\lambda}\beta}{s+\bar{\lambda}}} \qquad (34)$$

Multiplication of the numerator and denominator by $(s+\bar{\lambda})$ and division by ℓ^* yields

$$\frac{\delta n(s)}{\delta \mathscr{k}(s)} = \frac{s+\bar{\lambda}}{s^2 + (\bar{\lambda} + \frac{1-k}{\ell^*} + \frac{k\beta}{\ell^*})s + \frac{\bar{\lambda}}{\ell^*}(1-k)} \qquad (35)$$

The denominator is of quadratic form, and when average values of $\bar{\lambda} = 0.08$, $k = 0.5$, $\ell^* = 0.001$, and $\beta = 0.0064$ are substituted in the coefficient of s, it is seen that $\bar{\lambda}$ and $\frac{k\beta}{\ell^*}$ are negligible compared to $\frac{1-k}{\ell^*}$ so that

$$\frac{\delta n(s)}{\delta \mathscr{k}(s)} = \frac{s+\bar{\lambda}}{s^2 + (\frac{1-k}{\ell^*})s + \bar{\lambda}\frac{(1-k)}{\ell^*}} \qquad (36)$$

The roots of the denominator are found by use of the quadratic formula.

$$s = \frac{1 - k}{2\ell^*}\left\{- 1 \pm \left[1 - \frac{4\bar{\lambda}\,\ell^*}{1 - k}\right]^{\frac{1}{2}}\right\}$$

From the binomial expansion $(a \pm b)^n = a \pm nb$ ..... where $b \quad a$, the radical expands to $\left[1 - \frac{4\bar{\lambda}\,\ell^*}{1 - k}\right]^{\frac{1}{2}} \cong 1 - \frac{2\bar{\lambda}\ell^*}{1 - k}$ .... .
By substitution of the expanded terms for the radical, s becomes

$$s \cong \frac{1 - k}{2\ell^*}\left\{- 1 \pm \left[1 - \frac{2\bar{\lambda}\,\ell^*}{1 - k}\right]\right\}$$

First root

$$s_1 = \frac{1 - k}{2\,\ell^*}\left\{- 1 + 1 - \frac{2\bar{\lambda}\,\ell^*}{1 - k}\right\} = - \bar{\lambda}$$

Second root

$$s_2 = \frac{1 - k}{2\,\ell^*}\left\{- 1 - 1 + \frac{2\bar{\lambda}\,\ell^*}{1 - k}\right\} = - \left(\frac{1 - k}{\ell^*}\right) + \bar{\lambda}$$

When $\bar{\lambda}$ is considered negligible compared to the first term the resultant root is

$$s_2 = - \left(\frac{1 - k}{\ell^*}\right)$$

The denominator is now seen to be factorable to a good approximation into

$$(s + \bar{\lambda})\left(s + \frac{1 - k}{\ell^*}\right)$$

By substitution back into Equation 36 the result is

$$\frac{\delta n(s)}{\delta \alpha(s)} = \frac{s + \bar{\lambda}}{(s + \bar{\lambda})\left(s + \frac{1-k}{\ell^*}\right)} = \frac{1}{s + \frac{1-k}{\ell^*}} \qquad (37)$$

This is the final form of the transfer function. It shows that for a subcritical assembly one may ignore the effect of

the delayed neutrons in determining the change in neutron population due to a variation in the source. The terms containing the average delayed neutron decay constant cancel out, and thus the prompt neutron lifetime can be replaced by the average neutron lifetime. The assumption that the effect of the delayed neutrons can be ignored is valid for k_{eff} 0.995 (1). The subcritical assembly utilized in this investigation has a k_{eff} of about 0.52, hence the above assumption should be valid. The same result, Equation 37, is obtained from Equations 17 and 18 when the delayed neutron terms containing $\lambda_i c_i$ are deleted and the same derivation procedure as above followed.

Transfer Function with Reactivity Variation

Again utilizing Equation 17 and Equation 18 for the transfer function and Equations 22 and 23 for the steady state condition, let a small variation δk be imposed upon k so that

$$\begin{aligned} k &= k_o + \delta k \\ n &= n_o + \delta n \\ c_i &= c_{i_o} + \delta c_i \end{aligned} \tag{38}$$

where δk is the amplitude of the variation, and not the instantaneous value of the excess reactivity. Substitution of Equation 38 into Equations 17 and 18 yields

$$\frac{dn}{dt} = \frac{d\delta n}{dt} = \left[(k_o + \delta k)(1 - \beta) - 1\right]\frac{(n_o + \delta n)}{\ell^*}$$

$$+ pe^{-B^2\tau}\sum_{i=1}^{6} \lambda_i(c_{i_o} + \delta c_i) + s \qquad (39)$$

$$\frac{dc_i}{dt} = \frac{d\delta c_i}{dt} = \beta_i \frac{(k_o - \delta k)(n_o + \delta n)}{p\ell^* e^{-B^2\tau}} - \lambda_i(c_{i_o} + \delta c_i) \qquad (40)$$

By multiplication, setting products of small numbers equal to zero, and collecting the steady state terms of Equations 22 and 23 and equating them to zero one obtains

$$\frac{d\delta n}{dt} = \frac{n_o \delta k}{\ell^*} + \frac{k_o \delta n}{\ell^*} - \beta\frac{k_o \delta n}{\ell^*} - \beta\frac{n_o \delta k}{\ell^*}$$

$$- \frac{\delta n}{\ell^*} + pe^{-B^2\tau}\sum_{i=1}^{6}\lambda_i \delta c_i \qquad (41)$$

$$\frac{d\delta c_i}{dt} = \frac{\beta_i k_o \delta n}{p\ell^* e^{-B^2\tau}} + \frac{\beta_i n_o \delta k}{p\ell^* e^{-B^2\tau}} - \lambda_i \delta c_i \qquad (42)$$

By transformation to Laplace notation the equations become

$$s\,\delta n(s) = \frac{n_o}{\ell^*}\delta k(s) + \frac{k_o}{\ell^*}\delta n(s) - \beta\frac{k_o}{\ell^*}\delta n(s) - \beta\frac{n_o}{\ell^*}\delta k(s)$$

$$- \frac{\delta n(s)}{\ell^*} + pe^{-B^2\tau}\sum_{i=1}^{6}\lambda_i \delta c_i(s) \qquad (43)$$

$$\delta c_i(s) = \frac{\beta_i k_o}{p\ell^* e^{-B^2\tau}}\delta n(s) + \frac{\beta_i n_o}{p\ell^* e^{-B^2\tau}}\delta k(s) - \lambda_i \delta c_i(s) \qquad (44)$$

Solution of Equation 44 for $\delta c_i(s)$, substitution in Equation 43, and rearranging yields the transfer function

$$\frac{\delta n(s)}{\delta k(s)} = \frac{n_o}{k_o} \frac{1 - \beta + \sum_{i=1}^{6} \frac{\lambda_i \beta_i}{s + \lambda_i}}{\frac{s\ell^*}{k_o} + \frac{1}{k_o} - 1 + \beta - \sum_{i=1}^{6} \frac{\lambda_i \beta_i}{s + \lambda_i}} \tag{45}$$

The substitution of $\frac{\bar{\lambda}\beta}{s + \bar{\lambda}}$ for $\sum_{i=1}^{6} \frac{\lambda_i \beta_i}{s + \lambda_i}$ in Equation 45 yields

$$\frac{\delta n(s)}{\delta k(s)} = \frac{n_o}{k_o} \cdot \frac{1 - \beta + \frac{\bar{\lambda}\beta}{s + \bar{\lambda}}}{s\frac{\ell^*}{k_o} + \frac{1}{k_o} - 1 + \beta - \frac{\bar{\lambda}\beta}{s + \bar{\lambda}}} \tag{46}$$

The multiplication of numerator and denominator by $s + \bar{\lambda}$ and collection of terms yields

$$\frac{\delta n(s)}{\delta k(s)} = \frac{n_o}{k_o} \cdot \frac{s(1 - \beta) + \bar{\lambda}}{s^2(\frac{\ell^*}{k_o}) + (\frac{\bar{\lambda}}{k_o} + \frac{1 - k_o}{k_o} + \beta)s + \bar{\lambda}(\frac{1 - k_o}{k_o})} \tag{47}$$

Division of the numerator and denominator by ℓ^*/k_o yields

$$\frac{\delta n(s)}{\delta k(s)} = \frac{n_o}{k_o} \frac{\frac{k_o}{\ell^*} \left\{ s(1 - \beta) + \bar{\lambda} \right\}}{s^2 + (\bar{\lambda} + \frac{1 - k_o}{\ell^*} + \frac{\beta k_o}{\ell^*})s + \bar{\lambda}(\frac{1 - k_o}{\ell^*})} \tag{48}$$

This equation is seen to have the same denominator as Equation 35 which simplifies and factors to $(s + \bar{\lambda})(s + \frac{1 - k_o}{\ell^*})$. In the numerator the factor $(1 - \beta)$ is seen to be nearly equal to one when 0.0064 is substituted for β. Equation 48 then becomes

$$\frac{\delta n(s)}{\delta k(s)} = \frac{n_o/\ell^*}{s + \frac{1 - k_o}{\ell^*}} \tag{49}$$

which is the final form of the transfer function. This result

is the same as Equation 32 where the source strength was varied except for the constant multiplier n_o/ℓ^*. The average decay constant $\bar{\lambda}$ and fraction of delayed neutrons drop out of the final expression as before, showing that the transfer function for a subcritical assembly is independent of the delayed neutrons and dependent on the average neutron lifetime.

Modulus of the Transfer Function

Division of the transfer function, Equation 49, by $\frac{1-k_o}{\ell}$ and substitution of $S = j\omega$, yields

$$\frac{\delta n(s)}{\delta k(s)} = \frac{n_o/1-k_o}{1 + \frac{j\omega\ell}{1-k_o}} \tag{50}$$

The result of normalizing Equation 50 and setting it equal to $Y(j\omega)$ is

$$Y(j\omega) = \frac{\delta n(s)/n_o}{\delta k(s)/1-k_o} = \frac{1}{1 + \frac{j\omega\ell}{1-k_o}} \tag{51}$$

It is seen from Equation 51 that the prompt neutron break frequency, ω_p, is equal to $\frac{1-k}{\ell}$ for a subcritical assembly. ω_p effectively determines k for the subcritical assembly if ℓ is known, and the reverse is also true. The numerator and denominator are multiplied by the complex conjugate, $1 - \frac{j\omega\ell}{1-k_o}$, yielding

$$Y(j\omega) = \frac{1 - \frac{j\omega\ell}{1-k_o}}{1 + (\frac{\omega\ell}{1-k_o})^2} \tag{52}$$

The modulus of the transfer function, or the magnitude of $Y(j\omega)$, is

$$|Y(j\omega)| = \frac{\left\{(1)^2 + (\frac{\omega\ell}{1-k_o})^2\right\}^{\frac{1}{2}}}{1 + (\frac{\omega\ell}{1-k_o})^2}$$

which reduces to

$$|Y(j\omega)| = \frac{1}{\left\{1 + (\frac{\omega\ell}{1-k_o})^2\right\}^{\frac{1}{2}}} \tag{53}$$

The square of the modulus of the transfer function $|Y(j\omega)|^2$ is then

$$|Y(j\omega)|^2 = \frac{1}{1 + (\frac{\omega\ell}{1-k_o})^2} \tag{54}$$

The square of the modulus of the transfer function is the basis upon which the parameters of the transfer function can be evaluated as will be shown in the next section.

STOCHASTIC EVALUATION OF THE TRANSFER FUNCTION

The transfer function of an assembly can be determined experimentally by introducing sinusoidal variations in the input and measuring the phase angle and amplitude attenuation with frequency of the resulting sinusoidal variation in the output. This is usually accomplished by sinusoidally varying the strength of the neutron source or the reactivity and noting the resulting variation in the neutron flux. Variations in the neutron population due to the statistical nature of the fission process cause a change in reactivity and a fluctuation of the power level of a critical assembly. These random variations in the flux level may be considered as a summation of Fourier series which transform into Fourier integrals when the period approaches infinity (2). The transfer function of an assembly could then logically be extended to represent the response of a system to a random as well as sinusoidal input.

Consider a voltage which is a random or stochastic function of time and limited to a small range of frequencies between f_1 and f_2. One can determine a value which is proportional to the average power by squaring the function, integrating, and dividing the result by the time over which the integration was performed. If this "average power" is divided by $\Delta f = f_1 - f_2$, the frequency increment which the average power represents, the result is the average power or mean

THEORETICAL DERIVATION OF THE TRANSFER FUNCTION

The transfer function of an assembly can be determined experimentally by introducing sinusoidal variations in the input and measuring the phase shift and amplitude attenuation with frequency of the resulting sinusoidal variation in the output. This is usually accomplished by sinusoidally varying the strength of the neutron source or the reactivity and noting the resulting variation in the neutron flux. Variations in the neutron populations due to the statistical nature of the fission process cause a change in reactivity and a fluctuation of the power level of a critical assembly. These random variations in the flux level may be considered as a summation of Fourier series which transform into Fourier integrals when the period approaches infinity (2). The transfer function of an assembly could then logically be assumed to represent the response of a system to a random as well as sinusoidal input.

Consider a variable which is a random or stochastic function of time and limited to a small range of frequencies between f_1 and f_2. One can determine a value which is proportional to the average power by squaring the function, integrating, and dividing the result by the time over which the integration was performed. If this "average power" is divided by $\Delta f = f_1 - f_2$, the frequency increment which the average power represents, the result is the average power or mean

square voltage (amplitude) per unit frequency. This is called the power spectral density function. The term power spectral density function has been extended to apply to any function which consists of mean square signal amplitude per unit frequency of the band width investigated.

Nuclear reactions and fission processes which give rise to the neutron flux in a subcritical assembly can be considered as a random variable which has a normal or Gaussian distribution about some mean value of frequency of occurrence. The power spectral density of such a random variable is the average power (mean square signal amplitude) per unit frequency of the band width measured (2). It has the unique property of being a constant for this type of function and is defined as a "white noise". When such a random variable is passed through a linear system the output is a random variable which has been attenuated by the system characteristics (10).

If a system such as the subcritical assembly is excited by a white noise, which has a constant amplitude at all frequencies, one can analyze the output of the assembly over a range of frequencies to determine the response or transfer function (8). It has been shown mathematically that the output power density spectrum of a chain reacting system is proportional to the square of the modulus of the transfer function (11). This has also been demonstrated experimentally

for several nuclear reactors (4, 8).

Figure 1 shows an ideal system for power spectral density measurement in which it is assumed that the electronic components have perfect frequency response over the range of the investigation and introduce no noise. Under these conditions the system equation would be

$$G_{yy}(\omega) = G_{xx}(\omega)|Y(j\omega)|^2 = K|Y(j\omega)|^2 \qquad (55)$$

where $G_{xx}(\omega)$ = input power spectral density = constant.

$G_{yy}(\omega)$ = output power spectral density.

$Y(j\omega)$ = system transfer function.

$|Y(j\omega)|^2$ = square of modulus of transfer function.

Since the frequency response of the measuring equipment is not perfect, it also introduces a transfer function into the equation. This may be neglected and the response of the measuring equipment considered independent of frequency, if the break frequency of the equipment is beyond the range being investigated (8). The final form of the system equation was shown to be (8)

$$G_{yy}(\omega) = A + B|Y(j\omega)|^2 \qquad (56)$$

where A represents the level of measuring equipment noise and B represents the level of the assembly noise. The substitution of Equation 54 into Equation 56 yields

Figure 1. Ideal system for determination of output power spectral density function

$$G_{yy}(\omega) = A + \frac{B}{1 + (\frac{\omega \ell}{1-k})^2} \tag{57}$$

A sketch of Equation 57 is shown in Figure 2.

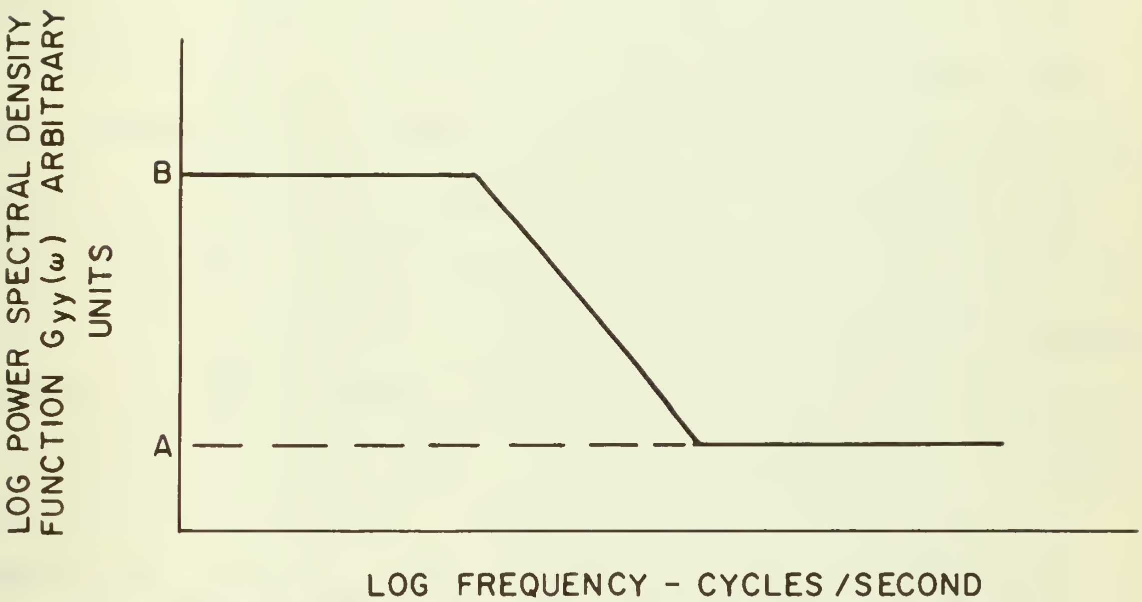

Figure 2. Ideal power spectral density function of an assembly

DESCRIPTION OF APPARATUS AND EXPERIMENTAL PROCEDURE

The graphite moderated subcritical assembly (14) utilized in this investigation was constructed at Iowa State University in 1957. Figure 3 is a photograph of the subcritical assembly with the end cover removed. The blocks were constructed from AGR grade graphite cylinders with diameters of 7.0 in. and 6 3/8 in., and length of 60 in. The lower nine layers were made up of blocks with a 6.0 inch square cross section and rounded corners of radius 3.5 inches. The top five layers were constructed of blocks with a 6.0 inch by 5.0 inch cross section with rounded corners of radius 3 3/16 inches. The density of the graphite was 1.56 gm. per cu. cm. or 97.3 lb. per cu. ft. An 8½ inch lattice was formed by placing uranium slugs in alternate channels as shown in Figure 3. The slugs of uranium were 1.000 in. in diameter and 8.00 in. in length and encased in aluminum cylinders 0.040 in. thick and with ends 0.20 in. thick. The outside dimensions were 1.080 in. in diameter and 8.40 in. in length. The uranium density was 19.0 gm. per cu. cm. or 1186 lb. per cu. ft.

The assembly was covered on the top and sides with a 0.010 in. sheet of cadmium sandwiched between a 3/8 in. sheet of plywood and a 1/8 in. sheet of masonite. An effective "black wall" for thermal neutrons was produced by the cadmium. The horizontal distances between the side sheets of cadmium was 60.5 in. and 62.5 in. With the extrapolation lengths

Figure 3. Front view of the subcritical assembly

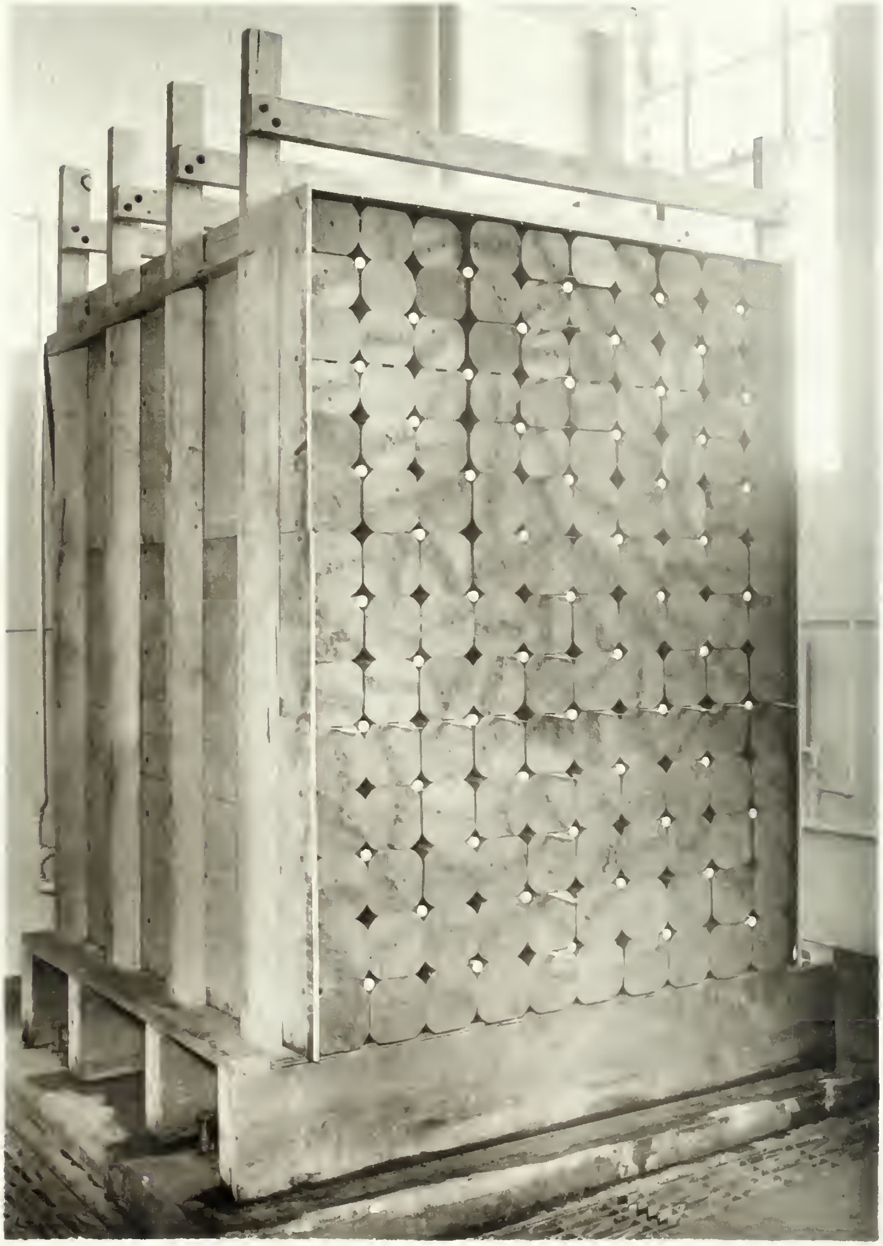

added, the effective size of the assembly was approximately 62 in. (side to side) by 64 in. (front to back).

The subcritical assembly was mounted on a pedestal as shown in Figure 3. The three spaces under the assembly housed 11.5 in. deep water tanks. The water provided protection from the neutron source which was mounted in the center tank under the pile.

The neutron source consisted of five individual plutonium-beryllium sources in containers 1 in. in diameter and 1 3/8 in. in length. The individual source strength was rated at one curie emitting approximately 1.63×10^6 neutrons per sec. The total source strength was 8.15×10^6 neutrons per sec. The five sources were mounted on a pedestal in the center tank which was filled with water. The sources were located on the centerline of the assembly directly below the bottom layer of graphite. Five holes were cut along the center line of the front panel of the assembly at one foot vertical intervals. The holes were cut to correspond to vacant channels in the lattice for insertion of the BF_3 neutron detector. The lowest hole, one foot above the bottom of the assembly, will be referred to as hole one, the hole two feet in height as hole two and so on.

The electronic circuitry for measuring the random variations in the neutron flux is shown in Figure 4. The neutron probe used was a Wood Counter Laboratory BF_3 detector. A

added, the effective size of the assembly was approximately 62 in. [illegible] 44 in. (given as [illegible]).

The subcritical assembly was mounted on a pedestal as shown in Figure 3. The three center [illegible] the assembly between 11.9 in. long water tanks. The water contained [illegible] from the neutron source which was mounted in the center tank below the pile.

The neutron source consisted of five individual plutonium-beryllium sources in containers 1 in. in diameter and 1 3/8 in. in length. The individual source strength was rated at one curie emitting approximately 1.63×10^6 neutrons per sec. The total source strength was 8.15×10^6 neutrons per sec. The five sources were mounted on a pedestal in the center tank which was filled with water. The sources were located on the centerline of the assembly directly below the bottom layer of graphite. Five holes were cut along the center line of the front panel of the assembly at one foot vertical intervals. The holes were cut to correspond to vacant channels in the lattice for insertion of the BF_3 neutron detector. The lowest hole, one foot above the bottom of the assembly, will be referred to as hole one, the hole two feet in height as hole two and so on.

The electronic circuitry for measuring the random variations in the neutron flux is shown in Figure 4. The neutron probe used was a Wood Chemical Laboratory BF_3 detector. A

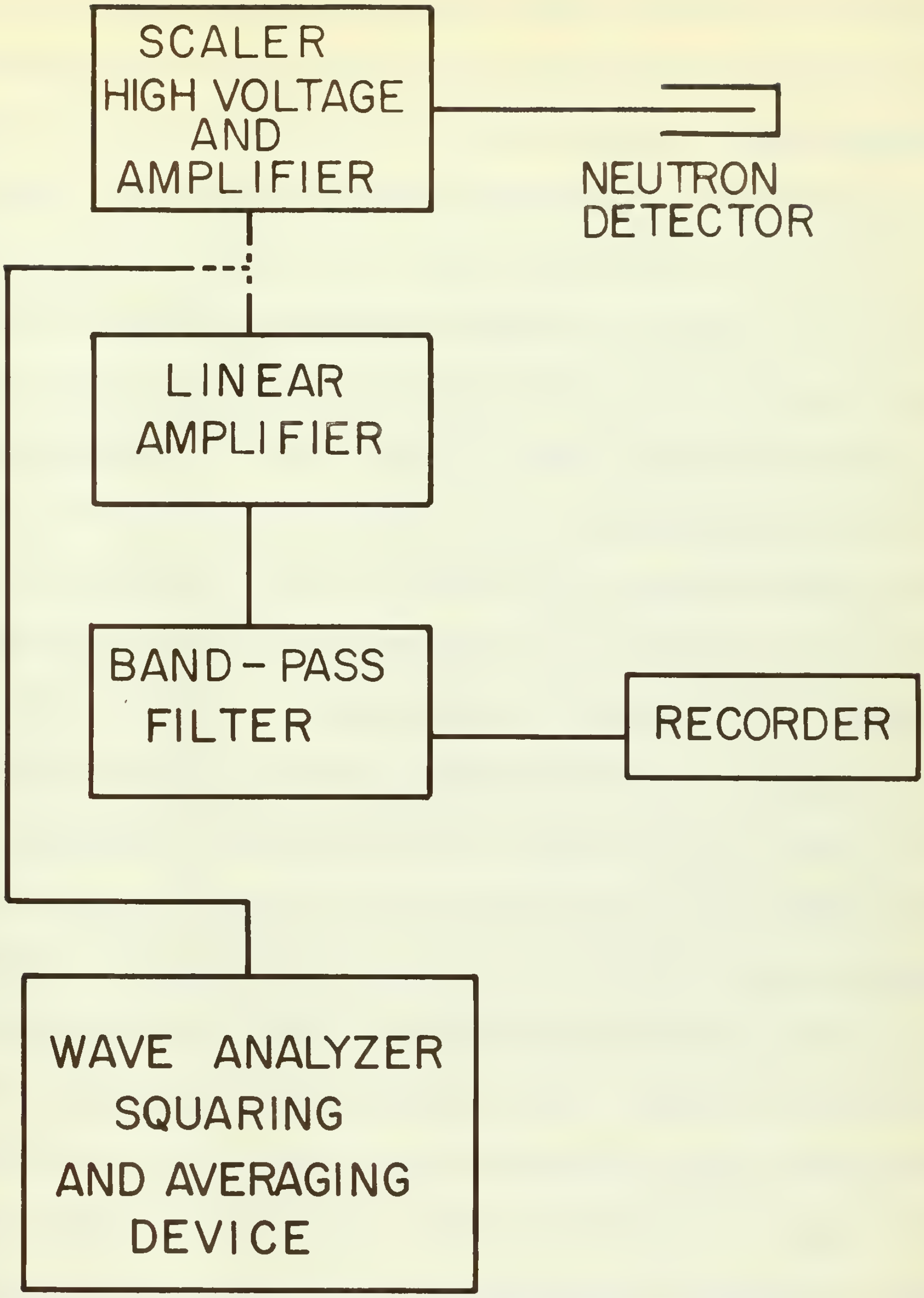

Figure 4. Electronic circuitry

Nuclear Chicago Ultrascaler Model 192A was used to supply high voltage to the detector and to amplify the signal from the detector. A Tektronix Type 112 Direct Coupled Amplifier with a flat frequency response from DC to 2 megacycles was used to further amplify the signal which was fed into a Khron-Hite ultra low frequency Band-Pass Filter, Model 330A. The band width of the filter was adjustable between a low cut off frequency of 0.02 cps to a high cut off frequency of 2000 cps. Frequency adjustment was accomplished by means of two dials calibrated with a logarithmic scale reading directly in cps from 2 to 20 and multiplying switches of 1/100, 1/10, 1, 10 and 100. A capacitance filter in the input circuit filtered out any DC component of the signal. The filter comprised an extremely low noise circuit, with internally generated hum and noise less than 100 microvolts. The filtered random signal was then fed into a two channel Brush Recorder Mark II for further amplification and recording. The recording pen sensitivity was variable from 0.01 to 10 volts per chart line, and the chart speed was variable from one to 125 mm per sec. This circuitry was used to investigate the frequency range of 0.02 cps to 20 cps. An alternate system was used for the frequency range of 20 cps to 100 cps and beyond, to facilitate data taking and processing. All of the components after the Nuclear Chicago Ultrascalar were replaced with a Hewlett-Packard Wave analyzer

Hewlett Packard [illegible] which was used to supply high voltage to the detector and to amplify the signal from the detector. A [illegible] with a flat frequency response from 10 to [illegible] was used to further amplify the signal which was fed into a Krohn-Hite variable band-pass filter, Model 330A. The band width of the filter was adjustable between a low cut frequency of 0.02 cps to a high cut off frequency of 2000 cps. Frequency calibration was accomplished by means of two dials calibrated with a logarithmic scale reading directly in cps from 2 to 20 and multiplying switches of 1/100, 1/10, 1, 10 and 100. A capacitance filter in the input circuit filtered out any DC component of the signal. The filter comprised an extremely low noise circuit, with internally generated hum and noise less than 100 microvolts. The filtered random signal was then fed into a two channel Brush Recorder Mark II for further amplification and recording. The recording pen sensitivity was variable from 0.01 to 10 volts per chart line, and the chart speed was variable from 1 to 125 mm per sec. This circuitry was used to investigate the frequency range of 0.02 cps to 50 cps. An alternate system was used for the frequency range of 50 cps to 100 cps and beyond, to facilitate data taking and processing. All of the components after the Hewlett Packard [illegible] were replaced with a Hewlett-Packard wave analyzer.

Model 300-A. The wave analyzer had an adjustable band pass of 30 cps to 145 cps, and a frequency range adjustable from zero cps to 16 kc. The output meter was graduated in RMS millivolts. Figure 5 is a photograph of the equipment described above.

Data were taken in each of the five holes, with the probe on the centerline of the assembly. The frequency range investigated was 0.02 cps to 100 cps. The circuitry including the band pass filter and recorder was used for the range of 0.02 cps to 20 cps. The wave analyzer was used from 20 cps to 100 cps. In order to minimize the introduction of spurious signals into the system, the output was taken from the scalar without the counting circuit being activated. The signal was then fed into the Tektronix Type 112 amplifier where the input and output signal was checked periodically with an oscilloscope to insure minimum a.c. pickup and no saturation of the amplifier. The signal was then passed through the band pass filter at a constant per cent band pass such as 0.02 cps to 0.04 cps, 0.04 cps to 0.08 cps, 0.08 cps to 0.16 cps, etc. The output of the band pass filter was recorded on both channels of the Brush recorder for two minutes for each band pass width setting. Typical random data for representative band pass widths are shown in Figure 6.

The power spectral density function for the 0.02 cps to 20 cps range was obtained for each band pass width by a method

Figure 5. Electronic equipment

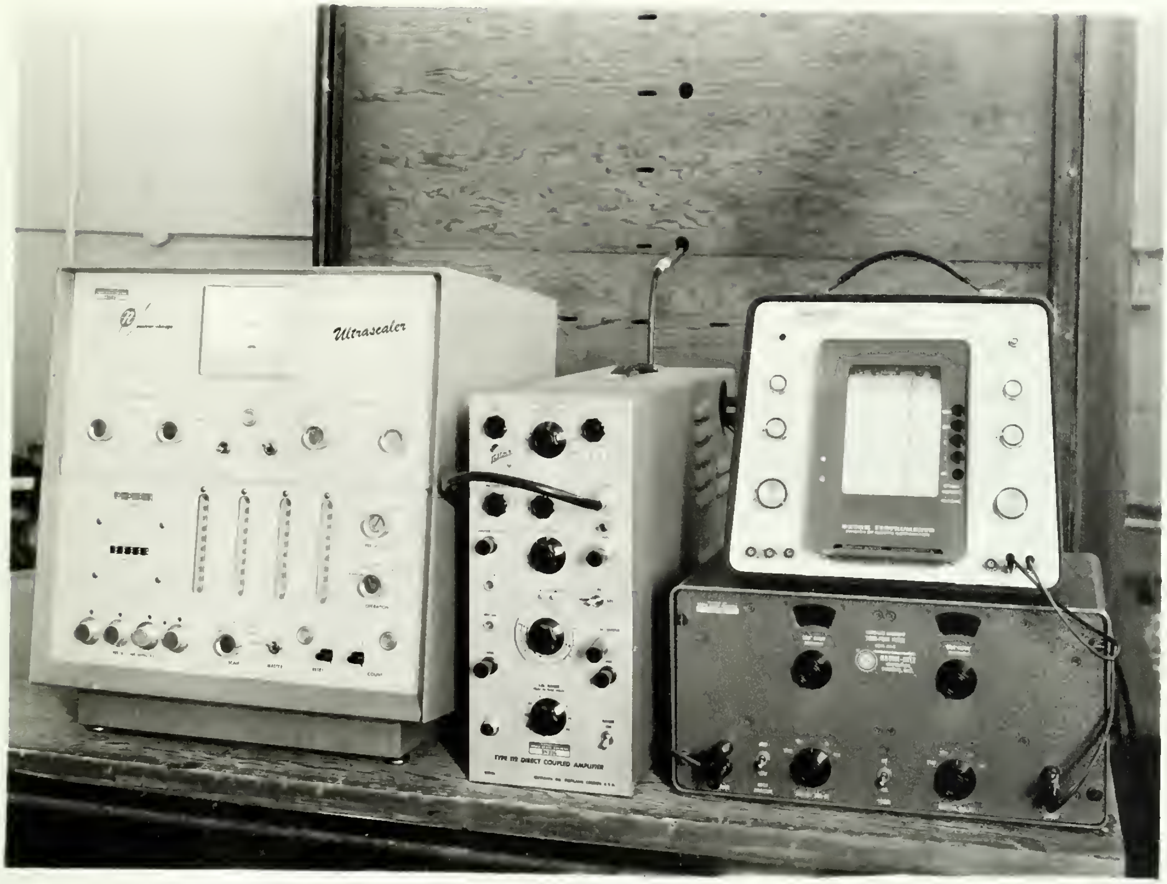
Ultrascaler
DIRECT COUPLED AMPLIFIER

Figure 6. Typical random data for representative band-pass widths

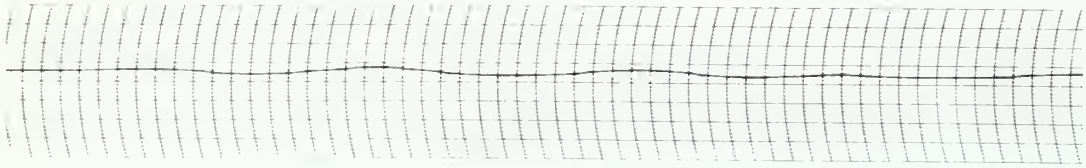

$\Delta f = 0.025$ cps

$\bar{f} = 0.0375$ cps

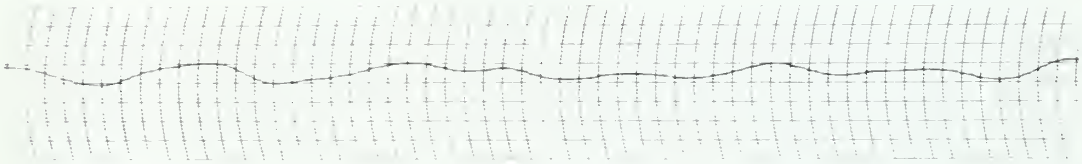

$\Delta f = 0.05$ cps

$\bar{f} = 0.075$ cps

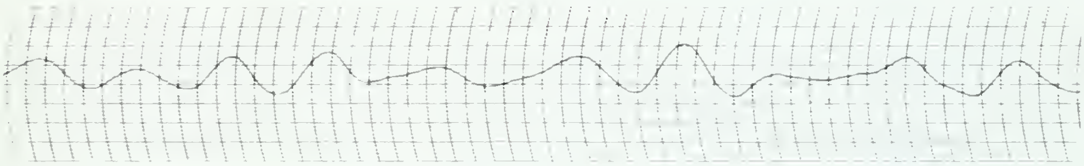

$\Delta f = 0.10$ cps

$\bar{f} = 0.15$ cps

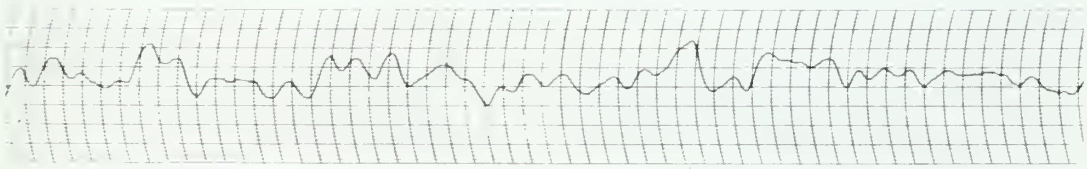

$\Delta f = 0.20$ cps

$\bar{f} = 0.30$ cps

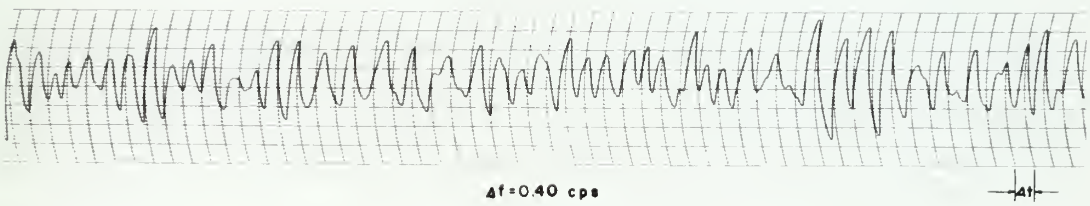

$\Delta f = 0.40$ cps

$\bar{f} = 0.60$ cps

All chart speeds 5 mm per sec $\Delta t = 1.0$ sec

similar to that outlined by Murphy (12). One hundred ordinates of each random trace were measured at one second intervals. Each ordinate was squared, and then the ordinates and their squares were summed separately and averaged. The variance, σ^2, was obtained by taking the difference between the average of the squared value and the square of the average value. This is equivalent to the average of the square of the difference from the mean.

$$\sigma^2 = (\overline{y^2} - \bar{y}^2) = \overline{(y - \bar{y})^2}$$

The power spectral density function $G_{yy}(\quad)$ was then obtained by dividing the variance by the band pass width in cps. This resulted in a value of mean square amplitude per unit frequency, or mean power per unit frequency, for the band width investigated.

$$G_{yy}(\omega) = \frac{\sigma_i^2}{\Delta f_i} \qquad \frac{\text{mean square amplitude}}{\text{unit frequency}}$$

The power spectral density for the 20 cps to 100 cps range was obtained by squaring the reading from the wave analyzer output meter. The meter read directly in RMS power per unit frequency of the band width investigated. By squaring the reading, the mean square amplitude or power per unit frequency of the band width investigated was obtained.

A sample calculation of the type used to reduce the data from the Brush recorder is included in the Appendix.

DISCUSSION OF RESULTS

The results of the data reduction are presented graphically in Figures 7 and 8 with the power spectral density, $G_{yy}(\omega)$, in arbitrary units versus frequency in cycles per second. The data were plotted only from 0.03 cps to 10.0 cps because the power spectral density appeared to become constant by 10.0 cps and remained a constant from 10.0 cps to 100 cps. This constant level represents the "A" term in Equation 57 which is the white noise of the instrumentation which is due primarily to the BF_3 detection chamber. The instrumentation noise decreases with increasing height in the assembly. This is explained by the fact that most of the instrumentation noise is due to the flux level or counting rate in the detection chamber which decreases with increasing height.

Figure 7 shows the change in power spectral density function along the axis of the assembly. For hole one (z = 1 ft) the power spectral density was determined to be approximately a constant throughout the range of frequencies investigated. This indicated that the random variations in the neutron flux were primarily due to the flux from the source which is "white noise". Hole two (z = 2 ft) shows a deviation from the constant power spectral density function of the instrumentation and indicates an increasing contribution from the fission flux and external source which have

Figure 7. Comparison of power spectral density function with height in the subcritical assembly

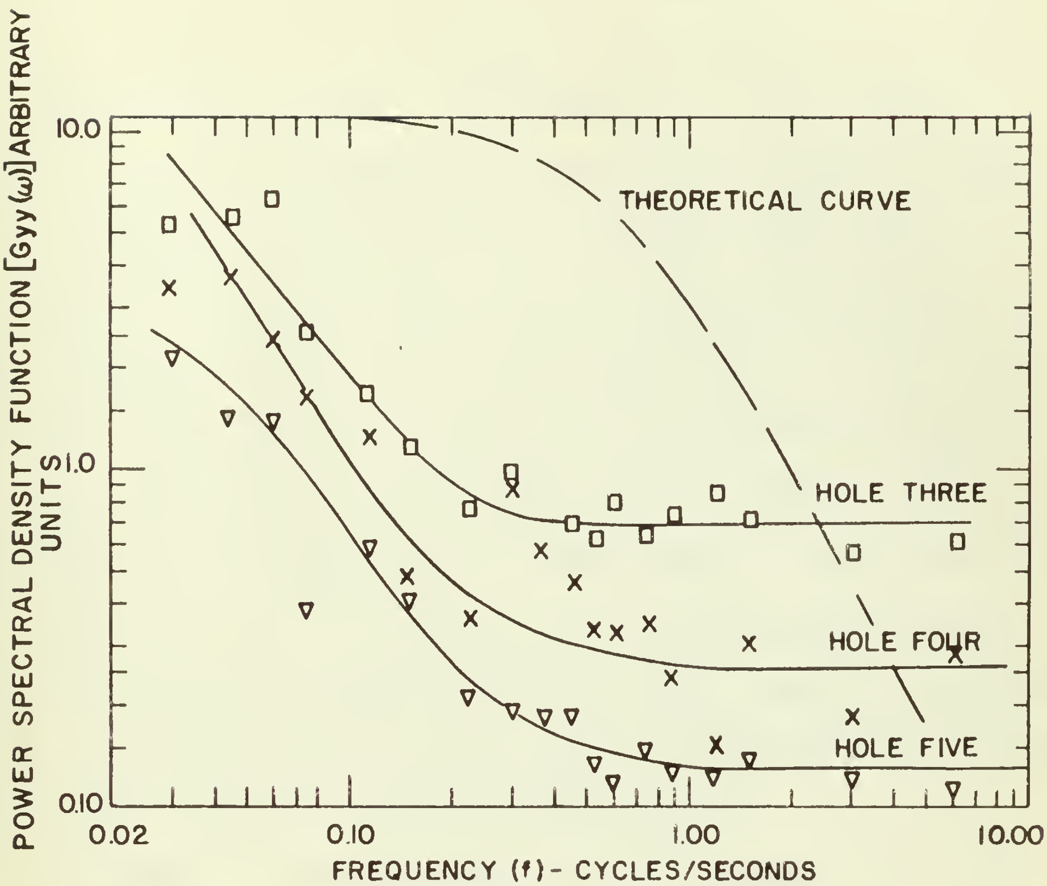

Figure 8. Comparison of measured with calculated power spectral density function

been attenuated by the transfer function of the assembly. Hole three ($z = 3$ ft) is 91.4 cm or approximately two diffusion lengths above the external source. The power spectral density function of the neutron flux at this level indicates that the transfer function of the assembly has operated on the flux to a much greater extent. Hole four ($z = 4$ ft) shows a maximum slope or attenuation of the power spectral density by the transfer function of the assembly. Hole five ($z = 5$ ft) shows a decreasing slope and a tendency to approach a break frequency toward the lower frequencies. This might be explained by a decrease in the "B" coefficient of Equation 57 which represents the level of assembly noise and is proportional to the square root of the power or flux level in the assembly. As "B" decreases, the instrumentation noise level approaches the assembly noise level, and the rounding off of the breaks in the curve tends to mask the true slope of the power spectral density function.

No definite break frequency was discernible from the data presented in Figure 7. The data for holes three, four, and five were replotted on Figure 8 along with a plot of the theoretical squared modulus of the transfer function from Equation 54. The theoretical equation was plotted using representative values of $\ell = 0.08$ sec and $k = 0.5$. Comparison with the theoretical curves shows the slope of the power

spectral density of hole four to be approximately the same as that for the theoretical curve.

CONCLUSIONS

The results were inconclusive because the neutron break frequency was not determinable and as a result it was not possible to evaluate the ratio $\frac{1-k}{\ell}$ exactly.

The best agreement between theory and experimental results was obtained at z = 4 ft = 122 cm. At this position, the slope of the attenuated power spectral density function was approximately the same as that predicted by theory. The value of the ratio $\frac{1-k}{\ell}$ was determined to be approximately 0.4/0.08 = 5.0. The results indicate that this ratio changes as z increases in value to beyond two diffusion lengths where it remains fairly constant until masked by the white noise of the detection chamber.

The evaluation of the transfer function of the subcritical assembly by analysis of the power spectral density shows promise and should be pursued further.

SUGGESTIONS FOR FURTHER STUDY

The plutonium-beryllium neutron sources utilized in this investigation were mounted on a pedestal beneath the assembly and were unmoderated except for the moderation by the graphite of the assembly. Interesting results might be obtained by encasing the sources in a block of paraffin moderator, and surrounding the moderated sources with graphite instead of the water shield. More significant results might be obtained by the use of a mechanical or electronic device for squaring and averaging the data. This means of data processing would allow much more rapid and accurate determination of the power spectral density, hence broadening the scope of investigation possible.

LITERATURE CITED

1. Axtmann, R. C., Dessauer, G., and Parkinson, T. F. Reactivity measurements in a subcritical pile. U.S. Atomic Energy Commission Report DP-48 [du Pont de Nemours (E. I.) and Co., Wilmington, Del.] November, 1955.

2. Bendat, J. S. Principles and applications of random noise theory. New York, N. Y., John Wiley and Sons, Inc. 1958.

3. Boland, J. F., Smith, R. R., and Rice, R. E. A measurement of the transfer function of a fast critical assembly. U. S. Atomic Energy Commission Report ANL-5782. [Argonne National Lab., Lemont, Ill.] Office of Technical Services. September, 1957.

4. Cohn, C. E. Measurement of prompt neutron lifetime by pile noise analysis. Argonne National Laboratory Memorandum RED-EPM-12 [Argonne National Lab., Lemont, Ill.] January 24, 1958.

5. Franz, J. P. Pile transfer functions. U. S. Atomic Energy Commission Report AECD-3260 [Technical Information Service, AEC] July 18, 1949.

6. Glasstone, S. Principles of nuclear reactor engineering. Princeton, N. J., D. Van Nostrand Co., Inc. 1955.

7. ________ and Edlund, M. C. The elements of nuclear reactor theory. Princeton, N. J., D. Van Nostrand Co., Inc. 1952.

8. Griffin, C. W. and Lundholm, J. G. Measurement of the SRE and KEWB prompt neutron lifetime using random noise and reactor oscillation techniques. U. S. Atomic Energy Commission Report NAA-SR-3765 [North American Aviation Inc., Downey, Calif.] October 15, 1959.

9. Harrer, J. M., Boyar, R. C., and Krucoff, D. Transfer function of Argonne CP-2 reactor. Nucleonics 10, No. 8: 32. 1952.

10. Laning, J. H. and Battin, R. H. Random processes in automatic control. New York, N. Y., McGraw-Hill Book Co. 1955.

11. Moore, M. N. The determination of reactor transfer functions from measurements at steady operation. U. S. Atomic Energy Commission Report NAA-SR-1972 [North American Aviation Inc., Downey, Calif.] August 15, 1957.

12. Murphy, G. J. Control engineering. Princeton, N. J., D. Van Nostrand Co., Inc. 1959.

13. Owens, J. I., Crever, F. E., and Pigott, J. H. A proposed automatic control system for the Schenectady reactor. U. S. Atomic Energy Commission Report AECD-4209 [Technical Information Service, AEC] March 29, 1949.

14. Ricci, W. J. Transfer function of a uranium graphite subcritical assembly. Unpublished M.S. Thesis. Ames, Iowa, Iowa State College Library. 1958.

15. Uhrig, R. E. Operating characteristics of a graphite moderated subcritical assembly. Nuc. Sci. and Eng. 5, No. 2: 120-126. 1959.

16. Velez, C. Autocorrelation functions of counting rate in nuclear reactors. Nuc. Sci. and Eng. 6, No. 5: 414-419. 1959.

ACKNOWLEDGMENTS

The author wishes to express his thanks to Dr. Robert E. Uhrig for his original suggestion of this investigation and for his valuable assistance along the way. Thanks are also due Dr. Glenn Murphy, Head of the Department of Theoretical and Applied Mechanics, and Chairman of the Nuclear Engineering Administrative Committee for making the facilities and equipment necessary for this investigation available. Dr. R. Grover Brown of the Department of Electrical Engineering assisted a great deal with many valuable suggestions concerning noise theory and data processing.

The author would like to express his gratitude to the U. S. Naval Postgraduate School and the Department of the Navy for making this educational opportunity possible.

APPENDIX

Sample calculations showing method of determining power spectral density.

Hole three (z = 3 ft)

$\Delta f = 0.4$ cps, $\bar{f} = 0.6$ cps

i	y_i	y_i^2
1	0.70	0.4900
2	-0.27	0.0729
3	0.70	0.4900
4	0.23	0.0529
5	0.40	0.1600
6	0.44	0.1936
7	1.25	1.5625
. . .	. . .	. . .
. . .	. . .	. . .
94	1.00	1.0000
95	-0.40	0.1600
96	0.43	0.1849
97	0.58	0.3364
98	1.30	1.6900
99	0.35	0.1225
100	0.90	0.8100

$\Sigma y_i = 56.89 \quad \Sigma y_i^2 = 63.8859$

$$\bar{y} = \frac{56.89}{100} = 0.5689$$

$$\bar{y}^2 = 0.323647$$

$$\overline{y^2} = \frac{63.8859}{100} = 0.638859$$

$$\sigma^2 = \overline{(y_1 - \bar{y})^2} = \overline{y^2} - \bar{y}^2$$

$$= 0.638859 - 0.323647$$

$$= 0.315212$$

$$G_{yy}(\omega) = \sigma^2/\Delta f = \frac{0.315212}{0.4} \cong 0.788 \ \frac{\text{mean square amplitude}}{\text{unit frequency}}$$